New Journal of Physics
The open access journal for physics

Metal–superconductor transition in low-dimensional superconducting clusters embedded in two-dimensional electron systems

D Bucheli[1,3], S Caprara[1,2], C Castellani[1,2] and M Grilli[1,2]

[1] CNISM and Dipartimento di Fisica Università di Roma 'La Sapienza', Piazzale Aldo Moro 5, I-00185 Roma, Italy

[2] Consiglio Nazionale delle Ricerche, Istituto dei Sistemi Complessi, Via dei Taurini, I-00185 Roma, Italy

E-mail: danielbucheli@hotmail.com

New Journal of Physics **15** (2013) 023014 (18pp)
Received 10 October 2012
Published 8 February 2013
Online at http://www.njp.org/
doi:10.1088/1367-2630/15/2/023014

Abstract. Motivated by recent experimental data on thin film superconductors and oxide interfaces, we propose a random-resistor network apt to describe the occurrence of a metal–superconductor transition in a two-dimensional electron system with disorder on the mesoscopic scale. We consider low-dimensional (e.g. filamentary) structures of a superconducting cluster embedded in the two-dimensional network and we explore the separate effects and the interplay of the superconducting structure and of the statistical distribution of local critical temperatures. The thermal evolution of the resistivity is determined by a numerical calculation of the random-resistor network and, for comparison, a mean-field approach called effective medium theory (EMT). Our calculations reveal the relevance of the distribution of critical temperatures for clusters with low connectivity. In addition, we show that the presence of spatial correlations requires a modification of standard EMT to give qualitative agreement with the numerical results. Applying the present approach to an $LaTiO_3/SrTiO_3$ oxide interface, we find that the measured resistivity curves are compatible with a network of spatially dense but loosely connected superconducting islands.

[3] Author to whom any correspondence should be addressed.

Contents

1. Introduction

Although two-dimensional (2D) electron systems have always been a topical subject in condensed matter physics, further renewed interest in this field has been triggered by the recent discovery of superconductivity at the metallic interface between two insulating oxide layers [1–4]. In addition, experiments on certain thin conventional superconducting films [5–8] reveal pseudogap effects, a phenomenon that could unveil new features of the superconducting transition in low-dimensional (low-D) disordered systems. In the particularly interesting cases of homogeneously disordered superconducting titanium nitride or indium oxide thin films, scanning tunneling spectroscopy data display inhomogeneities in the local density of states on mesoscopic spatial scales, clearly indicating the existence of an inhomogeneous superconducting state. Since tunneling experiments cannot directly access the 2D metallic layers at the oxide interfaces (although some attempts made on samples with very few top layers have detected interesting inhomogeneous textures [9]), magnetization and transport measurements are the only way to investigate these systems. Also in this case, evidence for an electronic phase separation has been found in $LaAlO_3/SrTiO_3$ (LAO/STO) layers [10]. Moreover, the sheet resistance curves $R_\square(T)$ near T_c, both in LAO/STO [2] and $LaTiO_3/SrTiO_3$ (LTO/STO) [3, 4] systems, show the peculiar feature of a marked tail on the low-temperature side.

Despite their differences, oxide interfaces and thin films often share the common feature of a broad superconducting transition. In a previous work [11], we investigated the possible origin of this pronounced width and found that superconducting fluctuations (alone) cannot account for its occurrence, while a model of global superconductivity arising from percolation of superconducting regions in the presence of quenched mesoscopic disorder can well produce the observed broad transitions. In this previous work, we also found that 'tailish' features can occur in the resistivity curves when disorder has spatial correlations. Specifically, while uncorrelated disorder can generically account for the pronounced width of the metal–superconductor transition, tails only occur when disorder displays a correlated character or when it occurs on nearly one-dimensional (1D) subsets of the system. We also found that the tailish resistivity can be obtained from a bimodal distribution of critical temperatures phenomenologically indicating that some parts of the system can have finite superconducting critical temperatures, while others can have very low or vanishing critical temperatures.

It is therefore important to understand how (correlated) disorder can act so as to give rise to the tailish resistivity because this feature can be a signature of specific physical mechanisms

at work in these systems. One natural possibility is that disorder correlations and/or nearly 1D (*filamentary*) structures arise in the system from nanofractures, topological defects such as crystal dislocations, steps, twinning domains and so on. In this regard, it was recently proposed that step edges on the surface of the STO substrate on which the LAO and LTO layers are grown can give rise to 1D metallic structures embedded in an insulating interface [12].

Percolative physics would also naturally emerge in the case of an inhomogeneous electronic reconstruction (phase separation) in which interface regions at different electronic filling are created, with the regions at higher filling possibly giving rise to a percolating superconducting cluster. Such a possibility of electronic phase separation has recently been proposed as the result of an intrinsic tendency of the interface to reconstruct differently due to substantial Rashba spin–orbit coupling of the electronic gas [13]. Of course, this intrinsic mechanism could easily cooperate and strengthen the effect of extrinsic defects.

Another possibility is that low-D superconducting subsets can spontaneously arise in the electronic gas even in the presence of homogeneously distributed disorder. In particular, one should remember that, besides fluctuations of the energy gap Δ, disorder can cause localization of electrons, transforming an otherwise metallic system into an insulator. If the metal is also a superconductor then at low temperatures, disorder can induce a superconductor–insulator transition [14–16][4]. In this case, a theoretical proposal has been put forward, which predicts that superconductivity at high disorder is maintained by coherence within a small set of preformed Cooper pairs. Consequently, in the vicinity of the superconductor–insulator transition, both the insulator and the superconductor contain these preformed Cooper pairs that either localize, leading to an insulating state, or condense into a coherent state with glassy behavior around the transition [14, 15, 17, 18]. The superconducting state then occurs on a small (filamentary) subset of the system, which forms in the electron gas around T_c with an important but rare path similar to the statistics of directed polymers [17, 18]. This picture is also supported by a theoretical analysis based on a disordered negative-U Hubbard model [19], where, at strong disorder, the current of the superconducting phase was found to flow along a low-D subset of the 2D lattice.

Therefore, both on phenomenological [11] and microscopic [12, 15, 17–19] grounds, the question naturally arises whether the tailish resistivity in LAO/STO and LTO/STO interfaces is due to the formation of a low-D superconducting cluster embedded in the 2D electronically reconstructed interface.

To shed light on the physics of these low-D superconducting clusters, we carry out a specific investigation of a 2D disordered metallic system represented by a random-resistor network (RRN). As in our previous work [11], the resistors represent mesoscopic metallic islands where superconductivity occurs at a local critical temperature T_c. The superconducting regions are assumed to be large enough to have a fully established local coherence and to make charging effects negligible. Mutual phase coherence immediately establishes between two neighboring superconducting islands, as soon as both become superconducting. This clearly distinguishes our framework from the case of granular superconductors, where the grains have usually nanoscopic sizes of the order of the coherence length of the pure system. We also stress that the matrix embedding the low-D superconductor is metallic so that our model, were it not for the role of phase fluctuations, bears some resemblance to the model of superconducting 'puddles' in a conducting metal [20]. The assumption of a metallic background seems to us

[4] For a discussion on possible scenarios of superconductor–insulator transition, see, e.g., [16].

appropriate because oxide interfaces (especially that of LTO/STO [3, 4]) do not show sizable temperature variations of the normal-state resistance as long as one is not too close to the superconductor–insulator transition.

To understand the effects of spatial (cluster) correlations, the resistances of our RRN are divided into two classes. The background matrix is formed by resistances which never become superconducting, embedding a cluster of resistances, each becoming superconducting below some local, randomly distributed T_c. These superconducting clusters are taken with spatially fractal-like distributions, which should describe the supposedly low-D character of the superconducting oxide interfaces, while keeping a rather 'dense' structure, as indicated by the moderately large mobilities of these interfaces and by the rather high slope of the resistivity near the transition. Since we are investigating transport properties, which could be crucially affected by the *long-distance* connectivity of the cluster, we explore different low-D structures. In particular, we will consider a diffusion-limited aggregation (DLA) and a symmetrized random walk (SRW) cluster (see below), which have similar dimensionality (and similar local connectivity), but are markedly different in long-range connectivity. In this way, we hope to highlight the specific role of (long-distance) connectivity for different low-D structures embedded in a 2D metal.

The paper is organized as follows. In section 2, we introduce the generic aspects of our model, while in section 3 we report the results of our numerical calculations for various kinds of low-D structures and of disorder distributions. Section 4 contains a discussion of the results and our concluding remarks.

2. The random-resistor model and effective medium theory

In [11], we considered a model of a 2D electron gas with mesoscopic defects as a square lattice whose bonds are assigned a random resistivity ρ_i. More precisely, each bond is assigned a local superconducting transition temperature $T_c^{(i)}$, extracted from a given distribution $\mathtt{W}\ (T_c)$, and the resistivity of the bond is written as $\rho_i = \rho_0\theta(T - T_c^{(i)})$, with the same high-temperature value ρ_0 on all bonds, $\theta(x)$ being the Heaviside step function. By decreasing the temperature T, more and more bonds become superconducting, and global superconductivity establishes as soon as a percolating superconducting path is formed in the system.

The simplest description of an RRN is provided by the effective medium theory (EMT) [21, 22], which is a mean-field treatment replacing the random resistors ρ_i with an effective medium resistivity ρ_{em} such that

$$\sum_i \frac{\rho_i - \rho_{em}}{\alpha\rho_i + \rho_{em}} = 0, \tag{1}$$

where the parameter α is related to the connectivity of the network. For a cubic network in D spatial dimensions, $\alpha = D - 1$.

In [11] (see [11] for further details), we used EMT as a benchmark and compared ρ_{em} with the exact numerical determination of the resistance of the RRN, obtained solving the Kirchhoff equations for the network in the presence of a difference of potential V between two opposite sides of an $N \times N$ square lattice. Once the current $I(T)$ flowing through the network at a temperature T is obtained, the resistance is found to be $R(T) = V/I(T)$. We showed that EMT provides a very good description of the temperature dependence of the resistivity, independently of the distribution of T_c, provided that disorder is spatially uncorrelated.

The solution of (1), specialized to our case, reads [11, 22]

$$\rho_{\rm em}(T) = (1+\alpha)\rho_0\theta(T - T_\alpha)\int_{T_\alpha}^{T} {\rm d}T_{\rm c}\, \mathtt{W}\ (T_{\rm c}). \tag{2}$$

Here, T_α is the critical temperature of the effective medium and is determined by

$$w_{\rm s}(T_\alpha) \equiv \int_{T_\alpha}^{+\infty} {\rm d}T_{\rm c}\, \mathtt{W}\ (T_{\rm c}) = \frac{1}{1+\alpha}, \tag{3}$$

where $w_{\rm s}(T) \equiv \int_{T}^{+\infty} {\rm d}T_{\rm c}\, \mathtt{W}\ (T_{\rm c})$ is the statistical weight of the superconducting bonds at a temperature T, measuring the frequency of occurrence of bonds with $T_{\rm c} > T$. From (2) it is readily seen that $\rho_{\rm em} \to \rho_0$ for $T \to \infty$ and $\rho_{\rm em}(T_\alpha) = 0$.

In the present paper, we consider a model in which the superconducting bonds only form a spatially correlated subset of the whole system. This subset provides a 'skeleton' network of bonds which become superconducting below a random local $T_{\rm c}^{(\rm i)}$, while the embedding system is a metal with temperature-independent resistive bonds. We shall explore the joint effects of the connectivity of the network and of the statistical distribution of the local critical temperature $\mathtt{W}\ (T_{\rm c})$. We shall mainly rely on the exact numerical solution of the Kirchhoff equations, but we shall refer to the EMT results to provide an interpretation of the outcomes of our calculations. When dealing with EMT, the presence of spatial correlations requires the introduction of an *effective* connectivity α, different from the standard connectivity.

3. Effects of low-dimensional disordered structures

3.1. The general framework

To investigate the effects of spatially correlated disorder, we consider the occurrence of a cluster where the zero-resistance state is carried by only a minor set of superconducting regions, reducing the effective dimension of the 2D electron gas near the superconducting transition. We disregard the physical origin (classical, such as due to mechanical stresses, non-uniform growth and so on, or quantum-mechanical, such as—for example—associated with the occurrence of coherence on a thin cluster of Cooper pairs near the superconductor–insulator transition) of this low-D superconducting 'skeleton' and we translate it into the framework of the RRN. Specifically, we consider an RRN on which low-D structures exhibiting strong spatial correlations and scale invariance are superimposed. Although the scale invariance is limited, once the structure is implemented on a finite lattice, this requirement leads to the formation of a rather dense cluster.

The fractal character of the cluster has no stringent physical grounds (even though it shares similarities with the theoretical arguments reported in [17, 18]), but is merely a technical way to produce rather dense subsets to represent strongly inhomogeneous systems with space correlations on a large scale.

Each bond of these spatially correlated clusters is given a critical temperature extracted from a probability distribution $\mathtt{W}\ (T_{\rm c})$, while the bonds not belonging to the 'fractal' cluster have fixed resistances ρ_0 (throughout the paper we take $\rho_0 = 1$). By varying the geometry of the clusters, as well as the probability distribution, the influence of these two aspects on the temperature dependence of the resistivity is studied. Note that in this approach the spatial distribution of superconducting bonds is considered to be independent of the probability

distribution of the critical temperatures. This is a simplifying assumption, made in the lack of a theory relating the mesoscopic inhomogeneity to the local superconducting temperature. It does allow, however, for a general and systematic analysis of the separate effects of geometry and of statistical distribution.

It is worth pointing out that in the previously considered models of uniform uncorrelated disorder [11], global superconductivity occurred as a true percolative phenomenon: upon lowering the temperature, more and more bonds became superconducting until a percolative cluster of superconducting bonds was reached. The geometrical support and the general features of this transition were typical of the percolation transition. On the other hand, in the present model the geometric support of bonds which can become superconducting is provided by a predetermined low-D subset of the network. When T is lowered, more and more bonds on this low-D support become superconducting and global superconductivity only occurs when a percolating path through the whole system is formed inside the filamentary subset. In this case, for instance, the dimension of the superconducting support is not due to pure percolation, but it clearly depends on the dimensionality of the supporting low-D subset.

In order to cover a different range of possible T_c distributions, we choose the two extreme cases of Gaussian and Cauchy statistics. The choice is motivated by their different asymptotic behavior: while the first has small tails and well-defined moments at all orders, the second is characterized by strong tails causing all moments except the mean to diverge. We take a Gaussian defined by the mean value μ_1 and variance σ,

$$\mathrm{W}\ (T_c) = \frac{1}{\sqrt{2\pi\sigma}} e^{-(T_c-\mu_1)^2/2\sigma^2} \tag{4}$$

and a Cauchy (i.e. Lorentzian) distribution defined by the mean value μ_2 and the width γ,

$$\mathrm{W}\ (T_c) = \frac{\gamma}{\pi[\gamma^2 + (T_c - \mu_2)^2]}. \tag{5}$$

Throughout the paper, the same parameters $\mu_1 = \mu_2 = 1$, $\sigma = 0.1$ and $\gamma = 0.08$ will be adopted. The parameters σ and γ are chosen so that the resistivity curves obtained with the Gaussian and Cauchy distributions have the same slopes close to the transition when space correlations are absent (figure 1).

As recalled in section 2, one of the findings of [11] was that *in the absence of space correlations* EMT performs remarkably well in reproducing the exact results of the RRN, irrespective of the specific T_c distribution. As an illustration, we report in figure 1 the resistivity curves of a uniform system obtained with the distributions here considered: the Gaussian (blue curves) and the Cauchy distribution (green curves). One notes that the resistance curves obtained with EMT (markers) match very well the exact numerical solutions (full lines). Thus, in the absence of correlations, EMT provides a useful tool to investigate the $\rho(T)$ dependence. In particular, the theory states that the resistivity of an RRN vanishes as soon as the weight of superconducting bonds w_s exceeds $1/(1+\alpha)$, where α is the connectivity of the system. In the present case of a uniform 2D lattice, $\alpha = 1$ and the percolation threshold at the transition yields $w_s = 1/2$. Referring to the resistance curves in figure 1, one notes that the critical temperature of the system is $T_\alpha = 1$, coinciding with the mean value of the (symmetric) distributions where half of the bonds have become superconducting. Thus, we correctly reproduce the predicted value of $w_s = 1/2$. At high temperature, the heavier tail of the Cauchy distribution results in a greater number of bonds with switched-off resistance. The resistivity for the Cauchy distribution

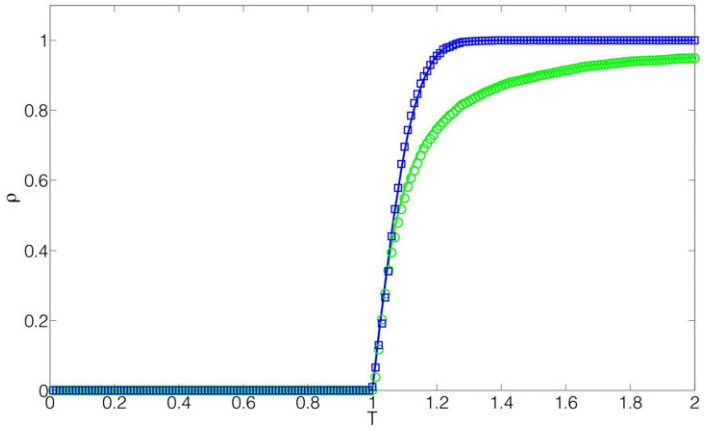

Figure 1. Resistivity curves of the uniformly disordered system. The blue curves correspond to a Gaussian distribution with $\mu = 1$, $\sigma = 0.1$ and the green ones to a Cauchy distribution with $\mu = 1$, $\gamma = 0.08$. The markers report the thermal evolution of the resistance obtained through the exact numerical calculations and the full lines the EMT solution.

remains smaller than that for the Gaussian distribution down to the establishment of global superconductivity on a percolating cluster.

To give a quantitative picture of the resistivity close to T_α, one can take the derivative of equation (2) defined in the framework of EMT:

$$\rho'_{\mathrm{em}}(T) = (1+\alpha)\rho_0 w \quad (T_c = T), \tag{6}$$

for $T \to T_\alpha$, which shows that the slope of the resistivity is proportional to the value of the distribution at equal temperatures. Combining this equation with the previous result $w_s(T_\alpha) = 1/2$, where the distribution has a maximum, one concludes that it is impossible to obtain 'tails' in the present case. In fact, due to the bell shape of the distributions the slope of the $\rho(T)$ is maximal at the mean value and thus also at the critical temperature of the system. By the same line of reasoning, one realizes that tailish behavior can be obtained even for a spatially uncorrelated distribution, in the very specific case of a symmetric bimodal distribution of T_c (see [11]). Here, we disregard this possibility and focus instead on the issue of space correlations. Quite importantly, our interest being devoted to transport properties, we will investigate the role of long-distance connectivity. In particular, we will consider two different low-D structures, which have similar short-distance connectivity (i.e. similar dimensionality and 'density'), but differing in their topology, which gives rise to substantially different long-distance connectivity.

3.2. Diffusion-limited aggregation

The first low-D cluster we implement is obtained through a simple growth process, generated by Brownian motion and known as *diffusion-limited aggregation*. Its construction is simple: a particle is released at the left edge of a 2D lattice and allowed to diffuse to the right. More precisely, the particle moves one bond to the right and then with equal probability one bond up or down. This procedure is iterated until the particle stops, as soon as it reaches the top, bottom or right edge, where it sticks. Then, other particles are launched in sequence and halted either when

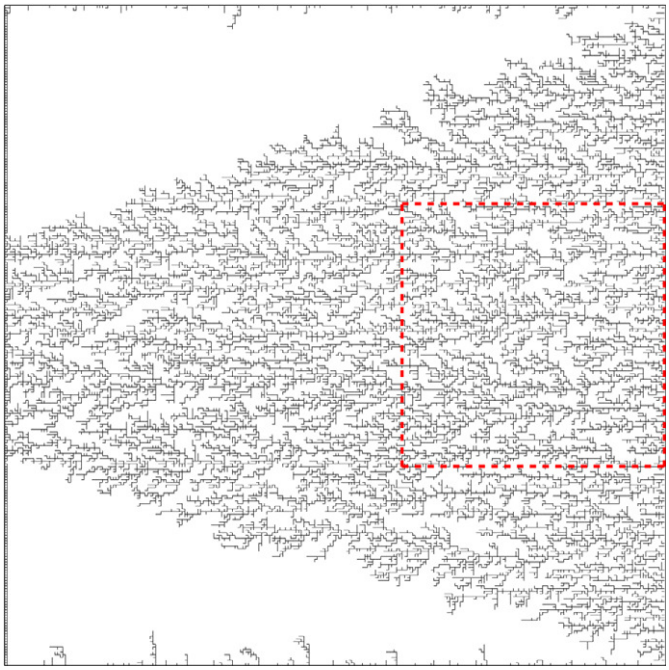

Figure 2. Spatial distribution of superconducting bonds obtained through DLA. The red square indicates the 100 × 100 lattice which is used for the calculations.

reaching one of the three edges or a bond already occupied by one of the previously diffused particles. The cluster obtained in a 250 × 250 square lattice after diffusing 50 000 particles is defined by the bonds where the particles stuck. Due to saturation at the left edge, the total number of superconducting bonds only amounts to about 25 000. Once this large cluster is obtained, we select a 100 × 100 sub-lattice as shown in figure 2 and perform the calculations for this smaller cluster. In this way, we try to model a more physical case where the low-D cluster covers the whole sample. So, henceforth we consider a 100 × 100 lattice, where only bonds belonging to the cluster are assigned a critical temperature T_c. The other bonds form a resistive background and are assigned the resistivity ρ_0 at all temperatures.

Figure 3 reports the resistance curves calculated on the 100 × 100 DLA cluster. We remark that for $T \gtrsim 1$ the curves for the Gaussian and Cauchy distributions are rather similar. Lowering the temperature, the system starts to exhibit stronger dependence on the specific statistics. In the Gaussian case, a percolating path is already formed around $T_\alpha = 0.78$, whereas for the Cauchy distribution one has to go as low as $T_\alpha = 0.33$ for the system to become fully superconducting. Examining the formation of the superconducting cluster, one finds that at T_α, the fractions of superconducting bonds are $w_s^G = 0.99$ and $w_s^C = 0.97$, respectively. So, practically all the bonds have to be superconducting in order for the phase transition to occur.

The reason for this strong condition lies in the very small set of percolating paths, i.e. the *effective* connectivity of the cluster is very close to zero. In other words, the cluster has rather marked 1D character and a few missing superconducting bonds are enough to prevent the system from percolating. To give a quantitative estimate of the effective connectivity of the cluster, we define the following measure (inspired by equation (3) defined in the EMT framework):

$$\alpha^{\text{eff}} = \frac{1}{w_s(T_\alpha)} - 1. \tag{7}$$

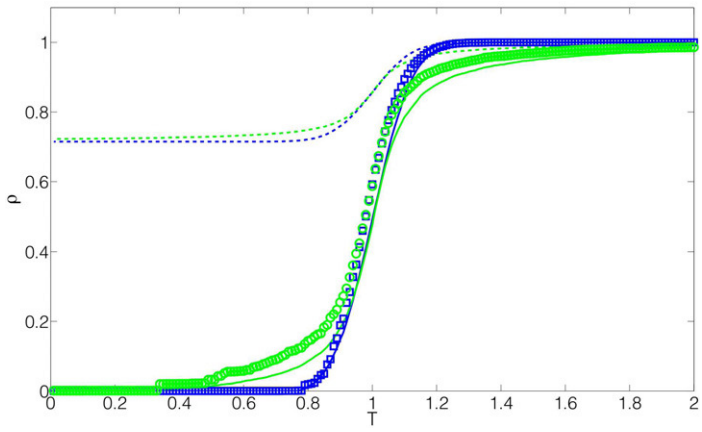

Figure 3. Resistivity curves of DLA cluster. The blue curves correspond to a Gaussian distribution with $\mu = 1, \sigma = 0.1$ and the green to a Cauchy distribution with $\mu = 1, \gamma = 0.08$. The markers report the thermal evolution of the resistance obtained by exact numerical calculations, the dashed lines by EMT on the system and the full lines by EMT on the cluster.

For instance, comparing $w_s^{U}(T_\alpha) = 0.5$ and $w_s^{G,DLA}(T_\alpha) = 0.99$, where the superscripts U and DLA refer to the case of a uniform and DLA superconducting cluster, respectively, one realizes that the statistical weight of the superconducting bonds close to the critical temperature T_α clearly depends on the geometry of the cluster and, in particular, on its effective connectivity. In addition, we shall show below that taking $\alpha_{DLA}^{eff} = 1/0.99 - 1 = 0.01$ the EMT *restricted to the cluster* produces $\rho(T)$ curves close to the exact results. Therefore, even though space correlations do not enter explicitly, (7) still provides a good estimate of an effective connectivity, once the relevant space correlations are accounted for by restricting EMT to the cluster. A second effect of the small set of percolation paths is a strong dependence on the specific realization of the distribution: two different realizations of the same distribution might be quite different. This effect is particularly severe for the Cauchy distribution, which has larger deviations from the mean. Since the Gaussian distribution, having small deviations from the mean, produces a superconducting cluster with an effective connectivity $\alpha_{DLA}^{eff} = 0.01$, we assume this value to be representative of the appropriate connectivity of the underlying DLA cluster. On the other hand, the realization of the Cauchy distribution of critical temperatures on the cluster in figure 2 is such that a percolating path forms at a finite temperature but calculations of $\rho(T)$ for different realizations of $\mathtt{W}$ (T_c) show that on average the phase transition does not occur. This result can be understood by noting that the Cauchy distribution has rather wide tails so that $w_s^{C}(T \to 0) \approx 0.025$. Thus the fraction of bonds which never become superconducting is substantial and, owing to the low connectivity of the DLA cluster (requiring $w_s^{DLA} = 0.99$), it may well happen that non-superconducting bonds prevent full percolation being established down to zero temperature.

This effect makes it apparent that, on correlated clusters, the low values of connectivity (like $\alpha_{DLA}^{eff} = 0.01$) render the system very sensitive to the statistics of the critical temperatures.

Figure 3 also shows that the EMT, when applied to the whole RRN (which is formed both by the low-D cluster and its complementary background), clearly misses the correct temperature dependence of the resistivity. According to its construction, outlined in section 2, this

mean-field-like theory neglects all spatial correlations and this discrepancy is expected. In addition, we remark that the decrease of ρ with T is a finite-size effect: as soon as spatial correlations are neglected what matters is the statistical weight of superconducting bonds only. This weight is smaller than (or equal to) N^D/N^2, which tends to zero for $N \to \infty$, leading to a vanishing drop of resistance when calculated by EMT on the whole system.

One can try to circumvent the shortcomings of EMT by evaluating it on the bonds belonging to the DLA cluster only. With this adjustment, the relevant space correlations can be taken into account using α^{eff}, and EMT reproduces quite accurately the main features of the exact solution: the regular behavior for $T > \mu$ and the stronger dependence on the distribution at low temperatures, due to the cluster's low connectivity. However, there is an overall shift from the restricted EMT solution with respect to the exact calculation. At high temperatures, where only a very few bonds have become superconducting, it is not favorable to force the current to flow through many resistive bonds simply to reach a few superconducting bonds. Therefore, the current still flows through the system in parallel (only locally perturbed by the few superconducting bonds present). By decreasing the temperature the superconducting cluster increases and, consequently, also the amount of current going through it. Close to the transition the shift then nearly vanishes because the resistive background ceases to play an important role. More precisely, the current is essentially carried by one or a few large quasi-percolating paths, which only need a few resistors to switch off in order to fully percolate. For these paths, it is immaterial whether they are embedded in a 2D (markers in figure 3) or simply a quasi-1D system (full lines in figure 3).

3.3. Symmetrized random walk

The topology of the DLA cluster considered in the previous section is characterized by a few backbones (forming connected paths between the two vertical edges of the lattice) and many dangling branches. Now, we explore a different situation in which the low-D geometry does not contain any dangling branches.

We modify the construction scheme of the DLA in the following way. Instead of keeping only the final position of the diffused particles, their entire trajectory is incorporated into the cluster. In addition, the particles are free to cross the paths of previously diffused particles. Launching 50 particles from each of the four edges and letting them diffuse perpendicular to the initial edge, a cluster of the form shown in figure 4 is obtained.

As was the case for the DLA, the resistance curves of the SRW shown in figure 5 are very similar for $T \sim 1$. The difference at higher temperatures originates from the difference in the distributions. Looking at the superconducting cluster formed at $T = 0.9$, one finds that the weights of superconducting bonds are $w_s^G = 0.84$ and $w_s^C = 0.79$, respectively. Interestingly, this difference has little effect on the resistivity. In fact, at this temperature, the size of the connected superconducting regions is of the order of ten bonds for both distributions. In this regime, having a few superconducting bonds more or less does not produce a noticeable difference in the resistivity.

This behavior clearly changes as one approaches the transition temperature. For T slightly larger than T_α the current is carried by long-range superconducting regions which lack only a few bonds to fully percolate. Inspection of the superconducting cluster growth reveals that the percolation threshold is reached as soon as $w_s^G(T_\alpha^G) = 0.92$ and $w_s^C(T_\alpha^C) = 0.90$. The closeness of these two values is again an indication that the threshold weight $w_s(T_\alpha)$ only depends on the

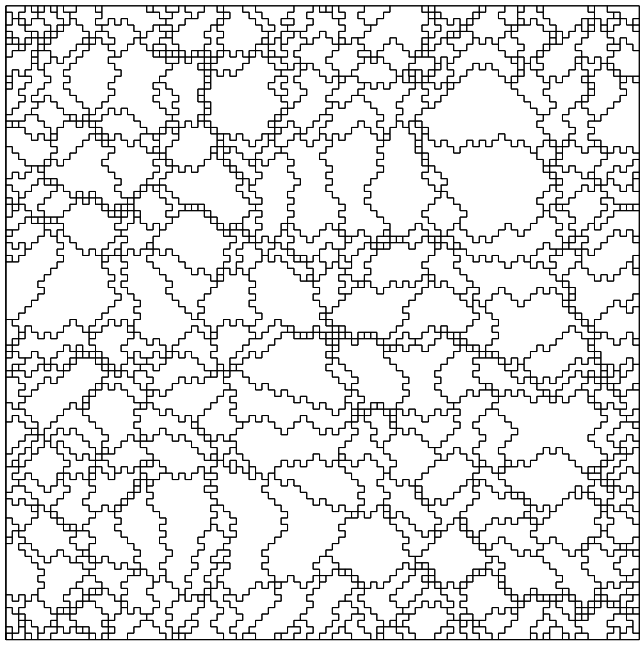

Figure 4. Spatial distribution of superconducting bonds obtained through an SRW on a 100 × 100 lattice.

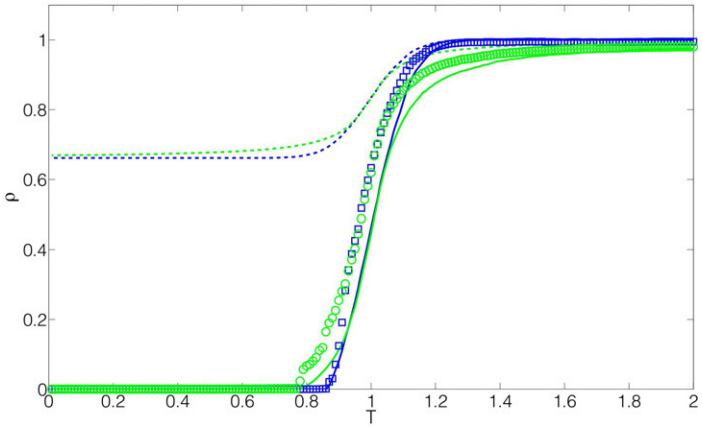

Figure 5. Resistivity curves of the SRW cluster. The blue curves correspond to a Gaussian distribution with $\mu = 1, \sigma = 0.1$ and the green to a Cauchy distribution with $\mu = 1, \gamma = 0.08$. The markers report the thermal evolution of the resistance obtained by exact numerical calculations, the dashed lines by EMT on the system and the full lines by EMT on the cluster.

'geometry' (i.e. the effective connectivity) of the underlying cluster and not on the specific T_c distribution. While the threshold is reached at $T_\alpha^G = 0.86$ in the first case, the heavy tail of the Cauchy distribution obliges the system to go as low as $T_\alpha^C = 0.76$ in the second case.

These considerations on w_s^U, w_s^{DLA} and w_s^{SRW} suggest that the high-temperature behavior is mainly determined by the dimensionality of the cluster. In fact, coarse-graining analysis using the box-counting method [23] shown in figure 7 reveals that the dimension of the clusters is

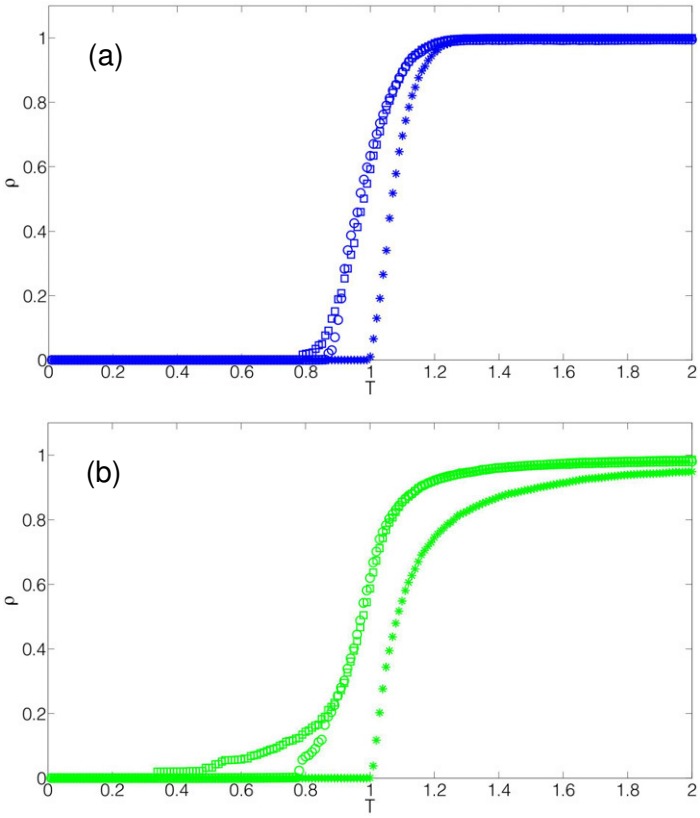

Figure 6. (a) Comparison of the resistivity curves for a Gaussian T_c distribution ($\mu = 1, \sigma = 0.1$) in a uniform system (stars), in an SRW cluster (circles) and in a DLA cluster (squares). (b) Comparison of the resistivity curves for a Cauchy T_c distribution ($\mu = 1, \gamma = 0.08$) in a uniform system (stars), in an SRW cluster (circles) and in a DLA cluster (squares).

$D^{\mathrm{DLA}} \approx D^{\mathrm{SRW}} \approx 1.8$. This is reflected in the congruence of $\rho^{\mathrm{DLA}}(T)$ and $\rho^{\mathrm{SRW}}(T)$ for $T > 0.9$, as well as in their leftward shift with respect to $\rho^{\mathrm{U}}(T)$ (with $D^{\mathrm{U}} = 2$), as is shown in figure 6.

In contrast, the calculation of the connectivity at the transition point reveals that $\alpha^{\mathrm{eff}}_{\mathrm{SRW}} \approx 0.1$. This value is much larger than in the DLA case ($\alpha^{\mathrm{eff}}_{\mathrm{DLA}} \approx 0.01$) signaling a substantially larger long-distance connectivity, but it is still relatively small. So, despite its 2D appearance, the low-temperature region, being more sensitive to the effective connectivity than to the dimensionality, behaves as quasi-1D. As far as the comparison between the EMT and the numerical exact results is concerned, the conclusions are analogous to the discussion given for the DLA cluster.

To develop a quantitative understanding of $\rho(T)$ close to the transition, we turn to an analytic approach based on a coarse-grained picture of the cluster. We consider the random walk cluster as a uniform system made up of large conducting segments containing $M \gg 1$ bonds. In the framework of EMT, the percolation threshold is reached when $1/2$ of the segments are superconducting. One can reformulate the condition in terms of the single bonds; since in order for a large segment to become superconducting, all its single bonds have to be superconducting,

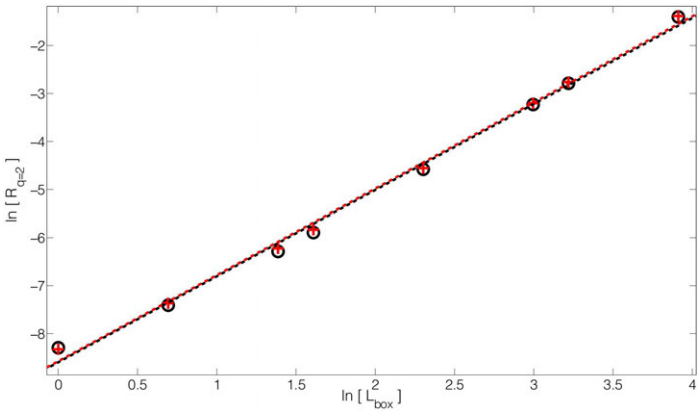

Figure 7. Determination of fractal dimension using the box-counting method: the lattice is subdivided into $N_{\rm box} = (N/L_{\rm box})^2$ boxes of size $A_{\rm box} = L_{\rm box} \times L_{\rm box}$. For each box k, we calculate the ratio $\mu_k = N^k_{\rm bond}/N_{\rm c}$, between the number of bonds belonging to the portion of the cluster inside this box $N^k_{\rm bond}$ and the total number of bonds belonging to the cluster $N_{\rm c}$. The quantity $R_q = \sum_{k=1}^{N_{\rm box}} \mu_k^q$ is then related to the box size according to $R_q = L_{\rm box}^{D(q-1)}$, where D is the fractal dimension. The figure shows a log–log plot with $L_{\rm box}$ varying from 1 to $N/2$ in the DLA cluster (circles) and in the SRW cluster (pluses). The dashed lines are linear regressions of $\ln R_{q=2} \propto D \ln L_{\rm box}$ in the DLA cluster (black line) and in the SRW cluster (red line): both lines have the same slope $D = 1.8$ and are hardly distinguishable.

one has

$$p^M = 1/2, \tag{8}$$

where p is the probability for a single bond to be superconducting. Close to the global critical point, the resistivity can be approximated by

$$\rho(T - T_\alpha) = C\rho_0 \left(\frac{1}{2} - p^M\right), \tag{9}$$

with $C > 0$. The purpose of the model is to analyze the possible occurrence of a tail in the resistivity curve, i.e. the behavior of the slope of $\rho(T)$ at $T \approx T_\alpha$:

$$\left.\frac{{\rm d}\rho}{{\rm d}T}\right|_{T \approx T_\alpha} = -Mp^{M-1}p', \tag{10}$$

where $C\rho_0$ was set to 1 for simplicity and $p' = {\rm d}p/{\rm d}T$. Since $T \approx T_\alpha$ and $M \gg 1$, the following approximations can be made:

$$p^M \approx \frac{1}{2}, \tag{11}$$

$$p \approx \exp\left(-\frac{1}{M}\ln(2)\right) \approx 1 - \frac{1}{M}\ln(2) \tag{12}$$

$$\Rightarrow M = \frac{\ln(2)}{1-p}. \tag{13}$$

Inserting the two expressions into (10), we obtain an expression for the derivative of the resistivity as a function of the single bond probability close to the critical point,

$$\left.\frac{\mathrm{d}\rho}{\mathrm{d}T}\right|_{T\approx T_\alpha} = -\frac{1}{2}\ln(2)\frac{p}{p(1-p)}, \tag{14}$$

$$\approx -\frac{1}{2}\ln(2)\frac{p}{1-p}, \tag{15}$$

$$= \frac{1}{2}\ln(2)\frac{W(T_c = T_\alpha)}{1-\int_{T_\alpha}^{\infty} W(T_c)\,\mathrm{d}T_c}. \tag{16}$$

In terms of the distribution the condition $p \approx 1$ (see (14)) means that the leading behavior is obtained taking the limit $W(T_c \to -\infty)$ (or, more precisely, $\mu - T_\alpha \gg \sigma, \gamma$; we point out that the critical temperature stays finite). This implies that the slope of the resistivity is proportional to the ratio of two small numbers. For the Gaussian distribution, the ratio is

$$\frac{W(T_c = T_\alpha)}{1-\int_{T_\alpha}^{\infty} W(T_c)\,\mathrm{d}T_c} \approx \frac{\frac{1}{\sqrt{2\pi}\sigma}\mathrm{e}^{-x^2}}{1-\left(1-\frac{\mathrm{e}^{-x^2}}{\sqrt{\pi}|x|}\right)}$$

$$= \sqrt{\frac{|x|}{2}}\frac{}{\sigma} \approx \frac{|T_\alpha - \mu_1|}{\sqrt{2}\sigma^2}, \tag{17}$$

where the shorthand notation $x = (T_\alpha - \mu_1)/\sqrt{2}\sigma$ was used. For the Cauchy distribution, the ratio is

$$\frac{W(T_c = T_\alpha)}{1-\int_{T_\alpha}^{\infty} W(T_c)\,\mathrm{d}T_c} \approx \frac{\frac{\gamma}{\pi[\gamma^2+(T_\alpha-\mu_2)^2]}}{1-\left(1-\frac{\gamma}{\pi T_\alpha}\right)}$$

$$\approx \frac{1}{|T_\alpha - \mu_2|}. \tag{18}$$

One observes that the slope for the Gaussian distribution depends linearly on the deviation from the critical temperature, while in the case of the Cauchy distribution the dependence is inversely proportional. Thus, for large M and comparable widths $\sigma \approx \gamma$, the slope in (17) is proportional to $|T_\alpha - \mu_1|/\sigma \gg 1$ and the slope in (18) is proportional to $\gamma/|T_\alpha - \mu_2| \gg 1$. This result highlights the strong influence of the distribution for low-D structures with $M \gg 1$.

4. Discussion

Our analysis is purely phenomenological in character: we embed a given low-D structure in a metallic environment, we impose a given T_c distribution on it and then we calculate the resulting resistivity curve. While this approach lacks any (possible, but not mandatory) microscopic connection between the geometrical and the T_c distribution, we separately access the distinct effects of these two ingredients.

As a first result, we point out that the geometrically correlated character of the superconducting clusters considered here greatly degrades the performance of the EMT mean-field-like approach. According to our experience in spatially uncorrelated disorder [11], this failure has nothing to do with the strength of disorder or the relative density of the

superconducting and the non-superconducting bonds, but is a mere result of space correlations. On the other hand, we showed that it is possible to find good qualitative agreement by restricting EMT to the cluster. In this case, one needs to introduce an effective connectivity (see (7)).

Calculating the standard (local) connectivity given by $\alpha = \langle z \rangle/2 - 1$, where $\langle z \rangle$ is the average number of nearest neighbors, we obtain $\alpha_{\mathrm{DLA}} = 0.38$ and $\alpha_{\mathrm{SRW}} = 0.15$, formally expressing the visual impression that the DLA cluster is 'denser' than the SRW. On the other hand, for the transport properties at issue in this paper it is important to have connected long-distance paths. In other words, the presence of regions with large internal connectivity is rather immaterial for transport if these regions are weakly connected to one another, thereby requiring the definition of an appropriate long-range connectivity [24]. Here, based on the EMT approach, we choose to introduce an effective connectivity to deal with a simple and 'handy' quantity immediately representing this average (i.e. long-distance) connectivity. Then, the comparison with $\alpha^{\mathrm{eff}}_{\mathrm{DLA}} = 0.01$ and $\alpha^{\mathrm{eff}}_{\mathrm{SRW}} = 0.1$ reveals that the effective connectivity is very different from the locally defined connectivity and formally translates the visual impression of different topological properties of the two clusters. However, despite this markedly different effective connectivity, one interesting finding of our work, reported in figure 6, clearly shows that, for a given T_{c} distribution, the different superconducting clusters display similar resistive behavior over most of the temperature range. This apparently contrasts with the finding of different effective connectivities (the effective connectivity of SRW is about ten times larger than the effective connectivity of the DLA cluster). This ineffectiveness of the connectivity is due to the metallic matrix, which carries a substantial part of the current unless the embedded cluster is (almost completely) superconducting. Only in these latter cases, near the global critical temperature at which percolation occurs (T_α), the current predominantly moves inside the almost completely superconducting cluster and its connectivity properties matter. One can then focus on this low-temperature region to pinpoint the specific role of this connectivity. Inspecting this part of figure 6 for the case of a Cauchy T_{c} distribution (b), one can make the following observations: both DLA and SRW clusters are low-D enough ($\alpha^{\mathrm{eff}}_{\mathrm{DLA}} = 0.01$ and $\alpha^{\mathrm{eff}}_{\mathrm{SRW}} = 0.1$) to display tailish behavior. This should be emphasized by the choice of the relatively long-tailed Cauchy distribution.

However, even in this more favorable case, the tail in the SRW case is much smaller than that of DLA. Furthermore, the DLA tail is even underestimated since the specific superconducting realization of the T_{c} configuration in figure 5 on the DLA is rather rare and in most realizations we found no complete superconductivity. This implies that going from the practically 1D connectivity of the DLA to the SRW with $\alpha^{\mathrm{eff}}_{\mathrm{SRW}} = 0.1$ is enough to largely suppress the tail. Therefore, our findings indicate that tailish resistances are only present when very few links determine the occurrence of long-distance connected paths (even large 'bulky' superconducting regions are immaterial near T_α if these are only very sparsely connected throughout the sample).

We also find that the effective connectivity is an intrinsic property of the cluster and is independent of the T_{c} distribution. This result is natural because upon reducing T, the T_{c} distribution only determines how 'fast' the resistances are switched off. However, this is irrelevant as far as the number of superconducting bonds needed to percolate is concerned.

Another interesting outcome of our analysis is that the effects of space correlations render the superconducting transition strongly dependent on the disorder distribution and, in particular, on its low-temperature asymptotics: as soon as percolation occurs through a quasi-1D path, the system needs to explore (almost) the entire T_{c} distribution, and thus becomes very sensitive to

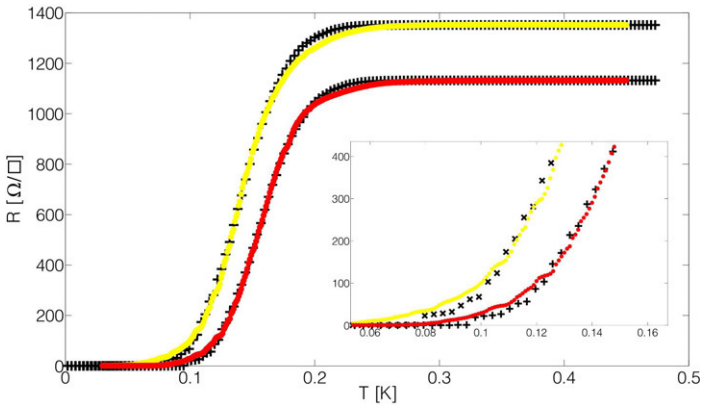

Figure 8. Fit of experimental resistance curves measured in the LTO/STO interface with a gate voltage V_G (see [4] for details) with theoretical curves obtained on a DLA cluster with a Gaussian distribution of T_c. The experimental data obtained for $V_G = 50\,V$ (yellow dots) are fitted with $\mu = 0.148\,K$, $\sigma = 0.033\,K$ (black crosses) and the data obtained for $V_G = 70\,V$ (red dots) are fitted with $\mu = 0.163\,K$, $\sigma = 0.031\,K$ (black pluses). Inset: enlarged view of the low-temperature behavior of $R(T)$.

its low-temperature part. This effect can be made particularly clear within the analytic approach of section 3.3, where the slope of the resistivity at T_α was shown to depend in inverse ways on the distance of T_α from the mean of the Cauchy or Gaussian distribution.

After the detailed analysis of the various effects of space correlations and T_c statistics, we come back to the initial question of whether and which of these aspects is relevant in explaining the tailish behavior of $\rho(T)$ in oxide interfaces. Based on the above results, we confirm that a rather dense but filamentary structure of superconducting bonds is a likely ingredient to account for a tailish resistivity. Due to their dimensionality, (i.e. larger than a purely 1D cluster), the clusters here considered are formed by superconducting bonds densely enough distributed to cause a linear decrease of the resistance with a relatively high slope, when lowering the temperature starting from the high-temperature metallic phase. In this regime, only the width of the statistical distribution of T_c matters, while none of the other details of the distribution play a significant role (as in a homogeneous cluster): the narrower the T_c distribution and the denser the support, the faster ρ decreases with T.

However, with further reducing the temperature, one gets close to the global critical temperature, where the global superconducting state appears via the percolative 'chaining' of superconducting regions *on the low-D support*. Here, the crucial property determining the shape of the transition is not the dimensionality but the effective long-distance connectivity α^{eff}. The filamentary (quasi-1D) behavior of the DLA and SRW clusters results in a more or less pronounced tail of $\rho(T \square T_\alpha)$. The details of the shape of the tail (e.g. the slope of $\rho(T)$ at percolation) are controlled by the low-temperature asymptotics of the T_c distribution.

Applying our approach to an LTO/STO interface [4], we show that it is possible to fit the experimental resistance curves with theoretical curves obtained on a DLA cluster with a Gaussian T_c distribution. Figure 8 shows that our model successfully reproduces the shape of $R_\square(T)$ measured in such interfaces: the linear decrease of the resistance with a relatively high

slope and the *tailish* behavior close to the global critical temperature. We note only a small mismatch around $T \sim 0.2$ K where the resistance starts to bend down.

We also remark that the fit with a Gaussian distribution on an SRW cluster, as well as a Cauchy distribution on both DLA and SRW clusters, does not produce satisfactory agreement with the experimental data. According to our theory, the actual interface might thus be composed of superconducting islands with a spatial distribution slightly denser than a DLA cluster (to account for the above-mentioned small mismatch around $T \sim 0.2$ K) but with a similar long-range connectivity and a Gaussian distribution of local critical temperatures.

In conclusion, our approach and results may provide a guideline for more refined models, which should take into account the physical mechanisms that rule, e.g., the intra-grain pair formation leading to a local T_c (Cooper pairs in the presence of quenched impurities [25], disordered bosonic preformed pairs [26] and glassy superconducting transition [17, 18]), and the emergence of the inhomogeneous metal–superconductor structure with coexisting metallic and superconducting islands with a *distribution* of T_c.

Eventually, with the insight gained from such microscopic considerations, e.g., the relation between the local T_c and the local high-temperature resistivity (which was kept constant in our analysis), the present approach could be refined and the results should be tested against the experimental findings.

Acknowledgments

We are indebted to N Bergeal, J Biscaras, C di Castro, B Leridon, J Lesueur and J Lorenzana for interesting discussions and useful comments. SC, CC and MG acknowledge financial support from 'University Research Project' of the 'Sapienza' University under no. C26A115HTN.

References

[1] Reyren N *et al* 2007 *Science* **317** 1196
[2] Caviglia A D *et al* 2008 *Nature* **456** 624
[3] Biscaras J, Bergeal N, Kushwaha A, Wolf T, Rastogi A, Budhani R C and Lesueur J 2010 *Nature Commun.* **1** 89
[4] Biscaras J, Bergeal N, Hurand S, Grossetête C, Rastogi A, Budhani R C, LeBoeuf D, Proust C and Lesueur J 2012 *Phys. Rev. Lett.* **108** 247004
[5] Sacépé B, Chapelier C, Baturina T I, Vinokur V M, Baklanov M R and Sanquer M 2008 *Phys. Rev. Lett.* **101** 157006
[6] Sacépé B, Chapelier C, Baturina T I, Vinokur V M, Baklanov M R and Sanquer M 2010 *Nature Commun.* **1** 140
[7] Sacépé B, Dubouchet T, Chapelier C, Sanquer M, Ovadia M, Shahar D, Feigel'man M and Ioffe L 2011 *Nature Phys.* **7** 239
[8] Mondal M, Kamlapure A, Chand M, Saraswat G, Kumar S, Jesudasan J, Benfatto L, Tripathi V and Raychaudhuri P 2011 *Phys. Rev. Lett.* **106** 047001
[9] Ristic Z, Di Capua R, De Luca G M, Chiarella F, Ghiringhelli G, Cezar J C, Brookes N B, Richter C, Mannhart J and Salluzzo M 2011 *Europhys. Lett.* **93** 17004
[10] Ariando *et al* 2011 *Nature Commun.* **2** 188
[11] Caprara S, Grilli M, Benfatto L and Castellani C 2011 *Phys. Rev.* B **84** 014514
[12] Bristowe N C, Fix T, Blamire M G, Littlewood P B and Emilio A 2012 *Phys. Rev. Lett.* **108** 166802
[13] Caprara S, Peronaci F and Grilli M 2012 *Phys. Rev. Lett.* **109** 196401

[14] Ma M and Lee P A 1985 *Phys. Rev.* B **32** 5658
[15] Feigel'man M V, Ioffe L B, Kravtsov V E and Yuzbashyan E A 2007 *Phys. Rev. Lett.* **98** 027001
[16] Feigel'man M V, Ioffe L B, Kravtsov V E and Cuevas E 2010 *Ann. Phys.* **325** 1390
[17] Ioffe L B and Mézard M 2010 *Phys. Rev. Lett.* **105** 037001
[18] Feigel'man M V, Ioffe L B and Mézard M 2010 *Phys. Rev.* B **82** 184534
[19] Seibold G, Benfatto L, Castellani C and Lorenzana J 2012 *Phys. Rev. Lett.* **108** 207004
[20] Spivak B, Oreto P and Kivelson S A 2008 *Phys. Rev.* B **77** 214523
[21] Landauer R 1978 *Electrical Transport and Optical Properties of Inhomogeneous Media* ed J C Garland and D B Tanner (New York: AIP) p 2
[22] Kirkpatrick S 1973 *Rev. Mod. Phys.* **45** 574
[23] Halsey T C, Jensen M H, Kadanoff L P, Procaccia I and Shraiman B I 1986 *Phys. Rev.* A **33** 1141
[24] For a review see e.g. Burioni R and Cassi D 2005 *J. Phys. A: Math. Gen.* **38** 45
[25] Finkelstein A M 1987 *Sov. Phys.—JETP Lett.* **45** 46
[26] Fisher M 1990 *Phys. Rev. Lett.* **65** 923